



Removal of methylene blue from aqueous solution by graphene oxide

Sheng-Tao Yang^{a,b}, Sheng Chen^a, Yanli Chang^a, Aoneng Cao^a, Yuanfang Liu^{a,b}, Haifang Wang^{a,*}

^a Institute of Nanochemistry and Nanobiology, Shanghai University, Shanghai 200444, China

^b Beijing National Laboratory for Molecular Sciences, College of Chemistry and Molecular Engineering, Peking University, Beijing 100871, China

ARTICLE INFO

Article history:

Received 22 November 2010

Accepted 27 February 2011

Available online 6 March 2011

Keywords:

Graphene oxide
Methylene blue
Absorption
Decontamination

ABSTRACT

Graphene oxide (GO) is a highly effective absorbent of methylene blue (MB) and can be used to remove MB from aqueous solution. A huge absorption capacity of 714 mg/g is observed. At initial MB concentrations lower than 250 mg/L, the removal efficiency is higher than 99% and the solution can be decolorized to nearly colorless. The removal process is fast and more efficient at lower temperatures and higher pH values. The increase of ionic strength and the presence of dissolved organic matter would further enhance the removal process when MB concentration is high. The results indicate that GO can be applied in treating industrial effluent and contaminated natural water. The implications to graphene-based environmental technologies are discussed.

© 2011 Elsevier Inc. All rights reserved.

1. Introduction

The dyes in effluents are of serious concern because of their adverse effects to human beings and the environment [1,2]. Besides, the colors of the dyes are easily recognized even at very low concentrations, making them highly visible and undesirable. Many technologies have been developed for dye removal from aquatic environments, including physical, chemical, and even biological approaches [1,2]. Among these approaches, absorption is regarded as an easy and economic process [3,4]. Various materials, such as commercial active carbon, natural materials, bioadsorbents, and wastes from agriculture, have been used for such processes [3,4].

The rapid development in nanotechnology sheds light on the wastewater treatment [5]. Nanomaterials have been studied for the absorption of metal ions [6], dyes [7], and antibiotics [8]. Although it was discovered just a few years ago, graphene and its derivatives have attracted tremendous research interests not only in electronics and energy fields [9,10] but also in environmental applications [11–14]. For example, we have reported that graphene oxide (GO) could be used for heavy metal removal [11]. Beyond that, graphene composites have been used for arsenic and dye removal [12–14].

Herein, we report that GO can be directly used as an effective absorbent for the decoloration of methylene blue (MB, Fig. 1), which is widely applied to dye cotton, wood, and silk. GO has a huge absorption capacity for MB, which is competitive with other high performance absorbents. The fast absorption process of MB onto GO is one advantage. The absorption capacity of GO is

regulated by many influencing factors, such as temperature, pH value, ionic strength, and dissolved organic matter (DOM) content.

2. Materials and methods

2.1. Materials

GO was prepared following the modified Hummers method [15–17]. The GO solution was centrifuged at 12,000 rpm for 10 min, and the residue was collected for the absorption experiments. The obtained GO sample was characterized by infrared spectroscopy (IR, Avatar 370, Thermo Nicolet, USA), X-ray photoelectron spectroscopy (XPS, Kratos, UK), atomic force microscopy (AFM, SPM-9600, Shimadzu, Japan), and transmission electron microscopy (TEM, JEM-200CX, JEOL, Japan).

MB was purchased from ACROS Organics (Catalog No. 414240250). It was used without further purification. Other chemicals, bought from Sinopharm Chemical Reagent Co., Ltd., China, are of analytical grade.

2.2. Absorption of MB by GO

GO (400 μ L, 1.500 g/L, pH 6) was mixed with 800 μ L of MB (pH 6, 0.188–1.000 g/L) by a vortex mixer. The suspension was incubated at 25 °C for 1 h and then centrifuged at 14,000 rpm for 20 min. The absorbance of the supernatant was recorded at 664 nm (Fig. 1). Unless noted specifically, the following absorption experiments were performed following the same protocol.

The equilibrium concentration (C_e) of MB was calculated referring to the calibration curve of MB. The equilibrium sorption capacity (q_e) of GO was calculated by $(C_0 - C_e)/C_{GO}$, where C_0 is the initial

* Corresponding author. Fax: +86 21 66135275.

E-mail address: hwang@shu.edu.cn (H. Wang).

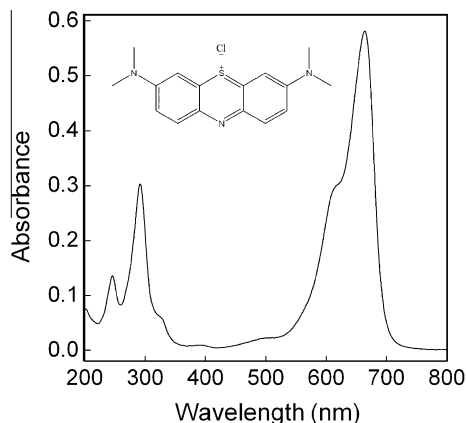


Fig. 1. Absorption spectrum and chemical structure of MB.

concentration of MB and C_{GO} is the final concentration of GO. The removal efficiency of MB was calculated by $(1 - C_e/C_0) \times 100\%$. The absorption data were fitted to both Langmuir model (Eq. (1)) and Freundlich model (Eq. (2)) (11). The maximum absorption capacity (q_m) and Freundlich constant (K_F) were obtained accordingly.

$$\frac{1}{q_e} = \frac{1}{q_m} + \frac{1}{bq_m C_e} \quad (1)$$

$$\ln q_e = \ln K_F + \frac{1}{n} \ln C_e \quad (2)$$

To demonstrate the removal efficiency directly, GO (2 mL, 1.500 g/L, pH 6) or deionized water was mixed with 4 mL of MB (0.312 g/L, pH 6). After the mixtures were incubated for 1 h and centrifuged, each supernatant was put into a vial for photography. Deionized water was taken as the reference.

2.3. The influence of contact time and temperature

To investigate the kinetics of the absorption, GO (400 μ L, 1.500 g/L, pH 6) was mixed with 800 μ L of MB (pH 6, 0.188–0.750 g/L), incubated at 25 $^{\circ}$ C for different time intervals, and then centrifuged at 14,000 rpm for 20 min. The concentration of MB (C_t) at different time points post mixture was measured for calculating the absorption capacity (q_t) by $(C_0 - C_t)/C_{GO}$.

The influence of temperature (0, 25, and 50 $^{\circ}$ C) on the absorption was investigated too. GO (400 μ L, 1.500 g/L, pH 6) was mixed with 800 μ L of MB (pH 6, 0.188–0.750 g/L), incubated at different temperatures for 1 h, and then centrifuged at 14,000 rpm for 20 min. The absorbance of the supernatant was recorded for q_e calculation.

2.4. The influence of pH, ionic strength, and DOM

As for the pH effect study, the initial pH of GO and MB was adjusted to 2–12 using NaOH or HCl aqueous solution. At each initial pH, GO (400 μ L, 1.500 g/L) was mixed with 800 μ L of MB (0.188–0.750 g/L) for 1 h and C_e was measured for the calculation of q_e .

Besides, the influence of ionic strength on the absorption was investigated. GO (400 μ L, 1.500 g/L, pH 6) was premixed with NaCl solution (200 μ L, pH 6, 0–600 mM), and then 600 μ L of MB (pH 6, 0.250–1.000 g/L) was added. The mixture was treated as described above for the calculation of q_e and the removal efficiency. As the corresponding control, NaCl solution (200 μ L, pH 6, 0, 150–600 mM), MB solution (600 μ L, pH 6, 0.250–1.000 g/L), and deionized water (400 μ L, pH 6) were mixed and treated the same way.

Because the pH and ionic strength may modulate the charge interaction between GO and EB, the ζ -potential of the GO under different conditions would be an important indicator of such interaction. Therefore, the ζ -potentials of GO (500 mg/L) under different pH values (2–12) and ionic strengths (pH 6, 0–100 mM Na⁺) were measured by a nanosizer (Nano ZS90, Malvern, UK).

Considering that DOM is common in aquatic environments, its effect on the absorption should be investigated. GO (400 μ L, 1.500 g/L, pH 6) was premixed with tannic acid solution (200 μ L, pH 6, 0–60 g/L), and then 600 μ L of MB (pH 6, 0.250–1.000 g/L) was added. The mixture was treated the same way for the calculation of q_e and removal efficiency. As the control, tannic acid solution (200 μ L, pH 6, 0–60 g/L), MB solution (600 μ L, pH 6, 0.250–1.000 g/L), and deionized water (400 μ L, pH 6) were mixed and treated the same way.

3. Results and discussion

3.1. Characterization of GO

The GO sample is readily dispersed in water forming brown suspension. The GO sheets, 300 nm~2.2 μ m in size, are mainly in a single-layer state according to the AFM investigation (around 0.9 nm in height) (Fig. 2a). Similar results are observed in the TEM image (Fig. 2b). The XPS spectrum of the GO sample suggests that the oxygen content is around 36% in mass. The IR analysis suggests that the oxygen atoms should be in the form of –COOH/–OH group (broad band around 3400 cm^{-1}) and C=O bond (1720 cm^{-1}) [11].

3.2. Absorption of MB by GO

The absorption isotherm of MB by GO is shown in Fig. 3a. At low C_e values, the absorption capacities (q_e) increase quickly. The q_e values increase slowly after C_e is above 150 mg/L. At C_e of 312 mg/L, the q_e value is 709 mg/g. When initial MB concentrations are lower than 250 mg/L, the removal efficiencies are higher than 99.4% and the remnant MB concentration is lower than 1.5 mg/L.

The photograph directly shows the successful decoloration of MB by GO (Fig. 3b). At initial MB concentrations of 200 mg/L, the decolorized solution is transparent and nearly colorless. The remnant MB in supernatant is only 0.3 mg/L, corresponding to a removal efficiency of 99.8%. Referring to the deionized water, only very faint blue color is recognized in the decolorized solution. In contrast, MB solution at 200 mg/L is dark blue and nontransparent. The very low remnant MB concentration might be regarded as a priority of absorption over other approaches. For example, after photocatalysis by TiO₂–graphene composites, there is still a considerable amount of MB in solution (~2 mg/L) [13]. Because it could decolorize MB solution in a wide concentration range, GO might be hopefully applied in treating not only the industrial effluent but also the contaminated natural water.

The absorption data of MB by GO fit the Freundlich model nicely (Fig. 4). The correlation coefficient R is 0.994. The absorption capacity is reflected by the K_F value of the Freundlich model, 469.6 mg/g (L/mg)^{1/n}. The n value is an indicator of the favorite state of the absorption process. Usually, when n is larger than 2, the adsorbent is regarded as a good one. Here, the n value is 13.4 for the absorption of MB by GO. Therefore, GO is an excellent adsorbent of MB. Besides, the $1/n$ value is close to 0, suggesting that the surface of GO is heterogeneous, which is consistent with the property of GO.

To compare the absorption capacity of GO with other adsorbents, we also fitted the data by Langmuir model, which is usually adopted in the studies of other adsorbents. However, the data were

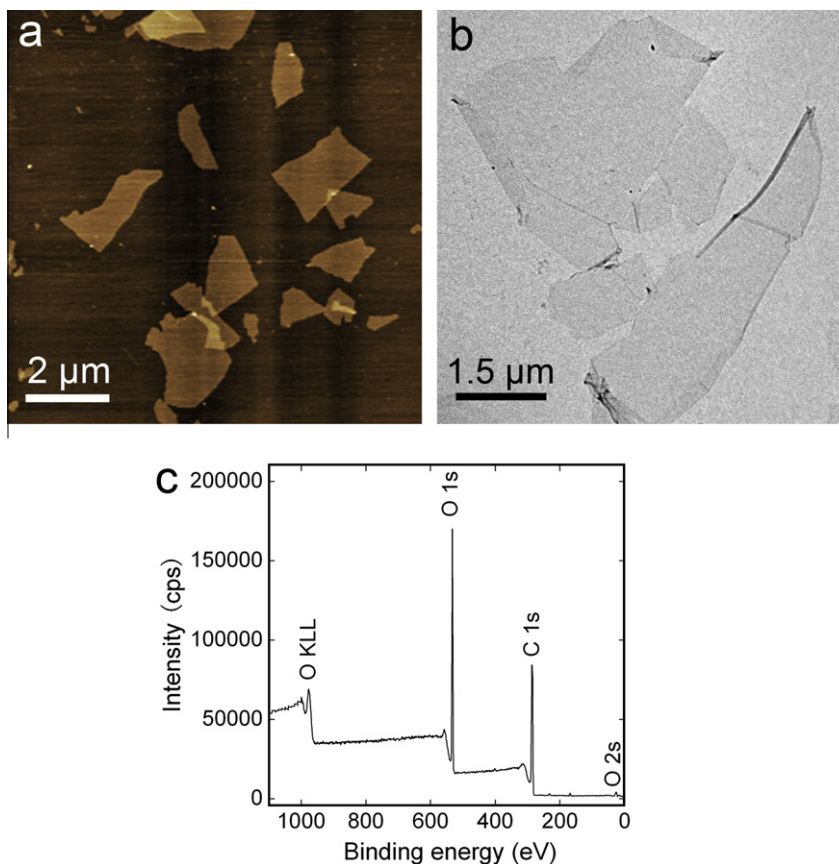


Fig. 2. Characterization of GO sample. (a) AFM image; (b) TEM image; (c) XPS spectrum.

not well fitted by the Langmuir model ($R = 0.903$). Thereupon, we fitted the last five data points (Fig. S1, $R = 0.984$), whose C_e values are higher than 30.2 mg/L, to obtain an approximate q_m value. The obtained q_m is 714 mg/g. The number is very close to the measured value (709 mg/g) at the C_e of 312 mg/L, indicating the dependability of q_m value. The q_m value of GO is competitive with that of other carbon-based adsorbents, such as active carbon, carbon nanotube (CNT), and graphene- Fe_3O_4 composite [18–23]. Table 1 summarizes the adsorption capacity of various adsorbents of MB. Due to the different surface and bulk properties, it is very difficult to perform a really fair comparison. Even though, our data still provide the useful information at least on the order of magnitude [11].

Chemically, there are plenty of oxygen atoms on GO in the forms of epoxy, hydroxyl, and carboxyl groups [24]. The oxygen atoms are highly amiable to positively charged molecules because of strong electrostatic interactions [11,25–30]. We have reported that GO sheets interact with Cu^{2+} intensely [11]. Other studies on graphite oxide have evidenced the strong interaction of oxygen atoms with cations and positively charged surfactants [25–30]. MB molecules are positively charged in nature, so the electrostatic interaction between the GO and the MB molecules is the primary binding strength. Such interaction has been adopted in fabricating graphite-MB composites [31].

There might be π - π stacking interaction contributing to the whole binding strength, too [32–34]. However, the literature suggests that the affinity of CNTs and MB is lower. The q_m of CNTs is only 6% of that of GO [7]. The major differences between CNTs and GO are the curvature of the structure and the oxygen content. The skeleton structure of both CNTs and GO sheets is a graphene structure, but the oxygen content of CNTs (commonly lower than

5 wt.%) [24,35] is much lower than that of GO. Separately, the absorption of MB onto expanded graphite was reported [36]. The skeleton structure of expanded graphite is nearly the same as that of GO, while the oxygen content of expanded graphite is much lower. The absorption capacity of MB on expanded graphite is three orders of magnitude lower than that on GO. These facts collectively suggest that the π - π stacking interaction only plays a minor role in the absorption of MB onto GO.

3.3. Influence of contact time and temperature

The absorption process of MB by GO reaches a balance very quickly (Fig. 5). In fact, MB-GO aggregates and precipitates immediately after the mixing. The fast absorption is one attractive merit of GO over other carbon-based MB adsorbents. For example, the absorption of MB onto active carbon and CNTs needs more than 1 h to reach a balance [7,19]. The currently presented kinetics data are still preliminary. More systematic investigations of the kinetics are very important and highly encouraged.

We also performed the absorption experiments under different temperatures to evaluate the influence of temperature. The absorption process is more favorable at lower temperatures, especially for a high MB concentration system (Fig. 6). At a MB concentration of 500 mg/L, the absorption capacity is 730 mg/g at 0 °C. When the temperature increases to 50 °C, the absorption capacity drops to 682 mg/g. This phenomenon implies that the absorption is an exothermic reaction. Actually, the environmental temperature could seldom be higher than 50 °C. Therefore, GO would be very effective under different environmental temperatures. To understand the thermodynamics of the absorption process, more efforts are required in the future.

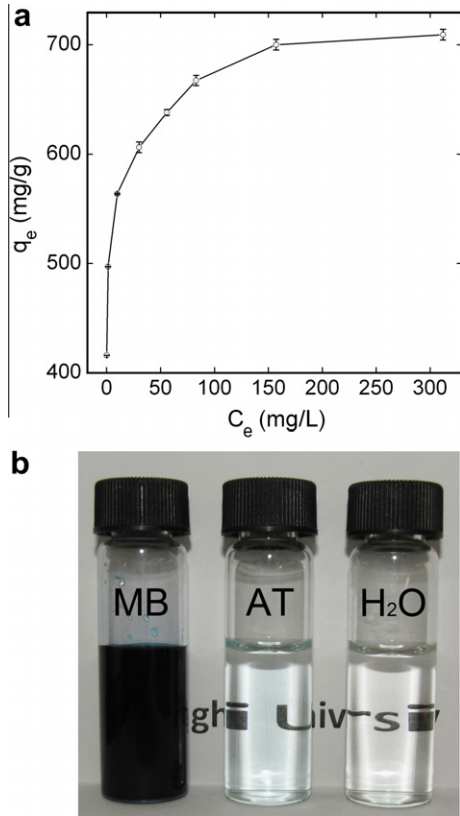


Fig. 3. Absorption of MB by GO at 25 °C. (a) absorption isotherm ($n = 3$); (b) photographs of the MB solution before (MB) and after (AT) the GO treatment.

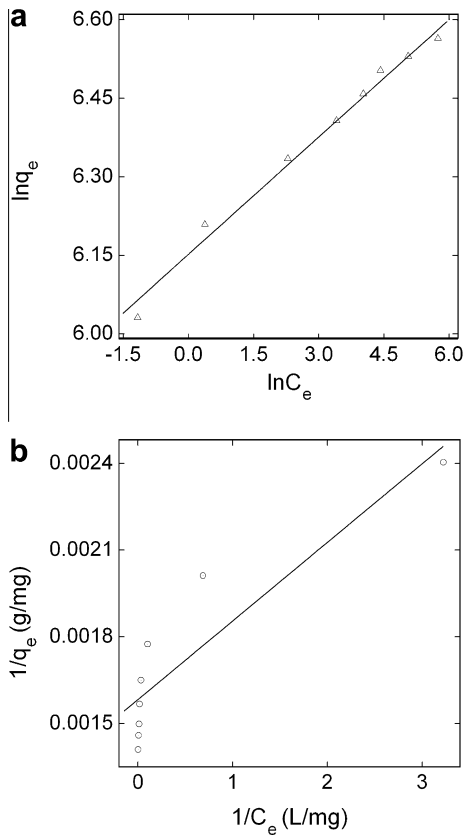


Fig. 4. Freundlich (a) and Langmuir (b) isotherms for the absorption of MB by GO.

Table 1
Maximum adsorption capacity (q_m) of various adsorbents of MB.

Absorbent	q_m (mg/g)	Refs.
Teak wood bark	914.6	[18]
Bamboo-based active carbon	454.2	[19]
Filtrisorb 400	476	[20]
Peat	323.7	[21]
Activated sludge biomass	256.4	[22]
Graphene-Fe ₃ O ₄ composite	190.1	[14]
CNTs	46.2	[7]
Clay	6.3	[23]
GO	714	This study

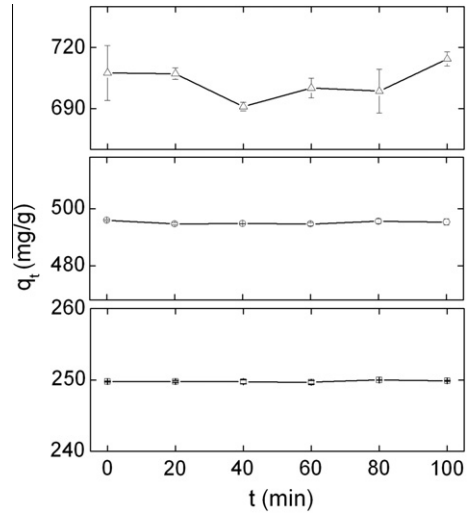


Fig. 5. The influence of contact time on the absorption of MB onto GO ($n = 3$). The initial concentration of MB: 500 mg/L (top), 250 mg/L (middle), and 125 mg/L (bottom).

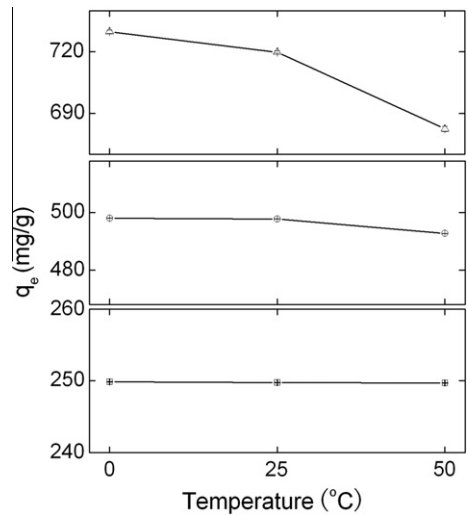


Fig. 6. The influence of incubation temperature on the absorption of MB onto GO ($n = 3$). The initial concentration of MB: 500 mg/L (top), 250 mg/L (middle), and 125 mg/L (bottom).

3.4. Influence of pH, ionic strength, and DOM

The pH regulates the ionization of both GO and MB, so it has significant influence on the absorption process. Generally, GO absorbs

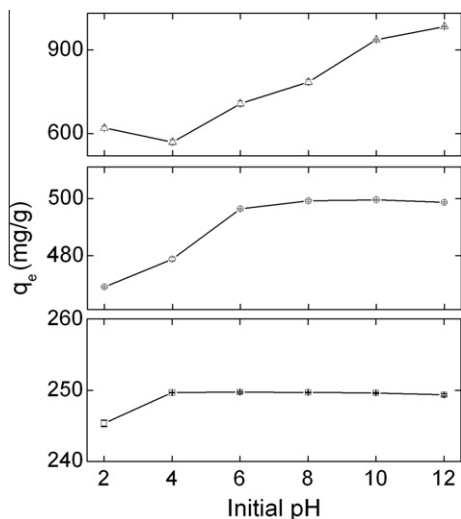


Fig. 7. The influence of pH on the absorption of MB onto GO ($n = 3$). The initial concentration of MB: 500 mg/L (top), 250 mg/L (middle), and 125 mg/L (bottom).

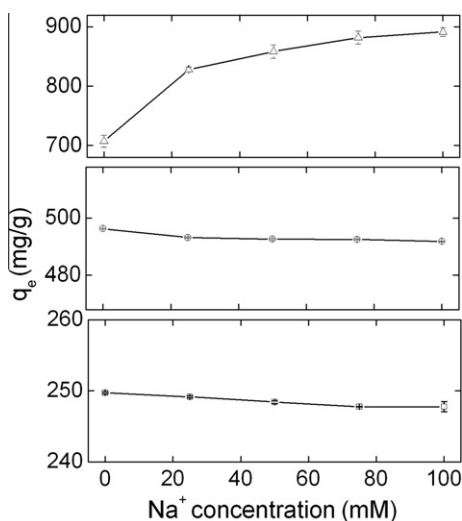


Fig. 8. The influence of ionic strength on the absorption of MB onto GO ($n = 3$). The initial concentrations of MB: 500 mg/L (top), 250 mg/L (middle), and 125 mg/L (bottom).

more MB at higher pH values (Fig. 7). At a MB concentration of 500 mg/L, the absorption capacity increases to 983 mg/g at pH 12. pH hardly affects the ionization of S-Cl of MB. However, at higher pH, GO is ionized and has more negative charges, which would enhance the electrostatic interaction of GO and MB. Such pH-regulated ionization is already reflected in the ζ -potential measurements, where GO shows a high negative ζ -potential at high pH values (Fig. S2). Moreover, the absorption process shifts the balance to a deprotonation direction to release more H^+ from carboxyl groups on GO. At higher pH, the released H^+ would be depleted by neutralization reaction, which makes the absorption more favorable. Similarly, the pH-regulated absorption behavior is also observed in the studies of other carbon absorbents [7].

The ionic strength regulates the absorption too. At high MB concentrations, the increase of the ionic strength leads to the increase of the absorption capacity (Fig. 8). At a MB concentration of 500 mg/L, the existence of 100 mM Na^+ makes the absorption capacity have a 26% increase. Sodium ions reduce the interaction of MB with H_2O , making it more amiable to GO. Sodium ions also

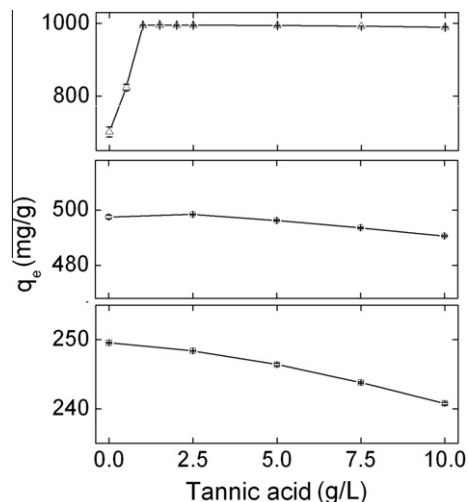


Fig. 9. Influence of DOM on the absorption of MB onto GO ($n = 3$). The initial concentration of MB: 500 mg/L (top), 250 mg/L (middle), and 125 mg/L (bottom).

depress the ionization of GO (Fig. S3). It seems that the increase of ionic strength improves the hydrophobicity of both MB and GO. The control experiment (in the absence of GO) suggests that the increase of ionic strength has little influence on the removal of MB by direct centrifugation (Fig. S4). At low MB concentrations, the capacity remains nearly unchanged.

In treating MB in natural water, the influence of DOM should be considered. Tannic acid is a widely used model molecule for DOM. We find that tannic acid has complicated effects on the absorption of MB onto GO (Fig. 9). At lower MB concentrations (125 and 250 mg/L), the increase of tannic acid content leads to the inhibition of absorption, resulting in a small decrease of the absorption capacity. The competitive absorption of MB onto GO and tannic acid (both GO and tannic acid are negatively charged) may contribute to the absorption inhibition.

At high MB concentration (500 mg/L), tannic acid promotes the removal significantly. The absorption capacity of GO increases to 990 mg/g, when the concentration of tannic acid reaches 10 g/L. This might be due to the additional formation of a MB-tannic acid complex, which is less charged and less soluble. The positive charges of MB molecules are neutralized by the negative charges of tannic acid molecules, therefore reducing the solubility of both MB and tannic acid. Although MB can be removed by tannic acid alone even in the absence of GO (Fig. S5), the removal efficiency is around 70% lower than that in the presence of GO. The tannic acid concentrations used here certainly are pretty high compared to the environmental level, and GO turns out to be very effective under such extreme conditions.

4. Conclusions

In summary, GO is an excellent absorbent for MB removal, with a maximum absorption capacity of 714 mg/g. At initial MB concentrations lower than 250 mg/L, the removal efficiency is higher than 99% and the solution can be decolorized to nearly colorless. The main strength of absorption is the electrostatic interaction, while the π - π stacking interaction might also contribute to the whole interaction. The removal efficiency is regulated by temperature, pH, ionic strength, and DOM content, especially at high MB concentrations. For future studies, the kinetics and thermodynamics of this absorption process should be systematically investigated. Our results certainly stimulate more interests and efforts on the graphene-based environmental technologies.

Acknowledgments

We acknowledge financial support from the China Ministry of Science and Technology (973 Project Nos. 2011CB933402 and 2009CB930200), the China Natural Science Foundation (No. 21071094), and Shanghai Leading Academic Disciplines (S30109).

Appendix A. Supplementary data

Supplementary data associated with this article can be found, in the online version, at [doi:10.1016/j.jcis.2011.02.064](https://doi.org/10.1016/j.jcis.2011.02.064).

References

- [1] T. Robinson, G. McMullan, R. Marchant, P. Nigam, *Bioresour. Technol.* 77 (2001) 247.
- [2] E. Forgacs, T. Cserhádi, G. Oros, *Environ. Int.* 30 (2004) 953.
- [3] G. Crini, *Bioresour. Technol.* 97 (2006) 1061.
- [4] M. Rafatullah, O. Sulaiman, R. Hashim, A. Ahmad, *J. Hazard. Mater.* 177 (2010) 70.
- [5] M.S. Mauter, M. Elimelech, *Environ. Sci. Technol.* 42 (2008) 5843.
- [6] G.P. Rao, C. Lu, F. Su, *Sep. Purif. Technol.* 58 (2007) 224.
- [7] Y. Yao, F. Xu, M. Chen, Z. Xu, Z. Zhu, *Bioresour. Technol.* 101 (2010) 3040.
- [8] L. Ji, W. Chen, S. Zheng, Z. Xu, D. Zhu, *Langmuir* 25 (2009) 11608.
- [9] A.K. Geim, *Science* 324 (2009) 1530.
- [10] C.N.R. Rao, A.K. Sood, K.S. Subrahmanyam, A. Govindaraj, *Angew. Chem., Int. Ed.* 48 (2009) 7752.
- [11] S.-T. Yang, Y. Chang, H. Wang, G. Liu, S. Chen, Y. Wang, Y. Liu, A. Cao, *J. Colloid Interface Sci.* 351 (2010) 122.
- [12] V. Chandra, J. Park, Y. Chun, J.W. Lee, I.C. Hwang, K.S. Kim, *ACS Nano* 4 (2010) 3979.
- [13] H. Zhang, X. Lv, Y. Li, Y. Wang, J. Li, *ACS Nano* 4 (2010) 380.
- [14] F. He, J. Fan, D. Ma, L. Zhang, C. Leung, H.L. Chan, *Carbon* 48 (2010) 3139.
- [15] W.S. Hummers Jr., R.E. Offerman, *J. Am. Chem. Soc.* 80 (1958) 1339.
- [16] N.I. Kovtyukhova, P.J. Ollivier, B.R. Martin, T.E. Mallouk, S.A. Chizhik, E.V. Buzaneva, A.D. Gorchinskiy, *Chem. Mater.* 11 (1999) 771.
- [17] A. Cao, Z. Liu, S. Chu, M. Wu, Z. Ye, Z. Cai, Y. Chang, S. Wang, Q. Gong, Y. Liu, *Adv. Mater.* 22 (2010) 103.
- [18] G. McKay, J.F. Porter, G.R. Prasad, *Water Air Soil Pollut.* 114 (1999) 423–438.
- [19] B.H. Hameed, A.T.M. Din, A.L. Ahmad, *J. Hazard. Mater.* 141 (2007) 819.
- [20] E.N. El Qada, S.J. Allen, G.M. Walker, *Chem. Eng. J.* 135 (2008) 174.
- [21] A.N. Fernandes, C.A.P. Almeida, C.T.B. Menezes, N.A. Debacher, M.D.D. Sierra, *J. Hazard. Mater.* 144 (2007) 412.
- [22] O. Gulnaz, A. Kaya, F. Matyar, B. Arikan, *J. Hazard. Mater.* 108 (2004) 183.
- [23] A. Gurses, S. Karaca, C. Dogar, R. Bayrak, M. Acikyildiz, M. Yalcin, *J. Colloid Interface Sci.* 269 (2004) 310.
- [24] D.R. Dreyer, S. Park, C.W. Bielawski, R.S. Ruoff, *Chem. Soc. Rev.* 39 (2010) 228.
- [25] C. Xu, X. Wang, L. Yang, Y. Wu, *J. Solid State Chem.* 182 (2009) 2486.
- [26] M. Machida, T. Mochimaru, H. Tatsumoto, *Carbon* 44 (2006) 2681.
- [27] H.H. Cho, K. Wepasnick, B.A. Smith, F.K. Bangash, D.H. Fairbrother, W.P. Ball, *Langmuir* 26 (2010) 967.
- [28] M. Sereych, T.J. Bandosz, *J. Colloid Interface Sci.* 324 (2008) 25.
- [29] Y. Matsuo, T. Niwa, Y. Sugie, *Carbon* 37 (1999) 897–901.
- [30] Z. Liu, Z. Wang, X. Yang, K. Ooi, *Langmuir* 18 (2002) 4926.
- [31] K. Haubner, J. Murawski, P. Olk, L.M. Eng, C. Ziegler, B. Adolphi, E. Jaehne, *ChemPhysChem* 11 (2010) 2131–2139.
- [32] S.-T. Yang, H. Wang, L. Guo, Y. Gao, Y. Liu, A. Cao, *Nanotechnology* 19 (2008) 395101.
- [33] X. Wu, S.-T. Yang, H. Wang, L. Wang, W. Hu, A. Cao, Y. Liu, *J. Nanosci. Nanotechnol.* 10 (2010) 6298.
- [34] F. Lu, X. Wang, M.J. Meziani, L. Cao, L. Tian, M.A. Bloodgood, J. Robinson, Y.-P. Sun, *Langmuir* 26 (2010) 7561.
- [35] Y.-P. Sun, K. Fu, Y. Lin, W. Huang, *Acc. Chem. Res.* 35 (2002) 1096.
- [36] M. Zhao, P. Liu, *Desalination* 249 (2009) 331.